HYDROLOGICAL CONNECTIVITY DOES CHANGE OVER 70 YEARS OF ABANDONMENT AND AFFORESTATION IN THE SPANISH PYRENEES

Manuel López-Vicente[1*], Estela Nadal-Romero[2,3], Erik L.H. Cammeraat[2]

[1] *Department of Soil and Water, Experimental Station of Aula Dei, EEAD-CSIC. Avda. Montañana 1005, 50059 Zaragoza, Spain*

[2] *Institute for Biodiversity and Ecosystem Dynamics (IBED), University of Amsterdam. P.O. Box 94240, 1090 GE Amsterdam, The Netherlands*

[3] *Department of Geography, Environmental Sciences Institute, University of Zaragoza. Pedro Cerbuna 12, 50009 Zaragoza, Spain*

[*] *Correspondence to: Manuel López-Vicente. E-mail: mvicente@eead.csic.es; mlopezvicente@gmail.com. Tel.: +34 976 71 61 24.*

Article history: Received: 17 February 2016; Revised: 11 April 2016; **Accepted: 11 April 2016**

Final version published online (http://onlinelibrary.wiley.com/doi/10.1002/ldr.2531/abstract): 31 May 2016, DOI: 10.1002/ldr.2531.

Wiley Online Library: ***Land Degradation & Development***. Edited By: Professor Artemi Cerdà; Impact Factor: **8.145**; ISI Journal Citation Reports © Ranking: 2015: **1/34 (Soil Science)**; **6/225 (Environmental Sciences)**. Online ISSN: 1099-145X.

ABSTRACT

Runoff connectivity depends on topography, rainfall, man-made elements (terraces, trails, roads, drainage systems) and vegetation. In this study we quantified the effects of 70 years of human activities on runoff connectivity in the mountaineous Araguás afforested sub-catchment (17.2 ha; Central Spanish Pyrenees). The IC index of hydrological connectivity was chosen to perform this metric over 6 land use scenarios at high spatial resolution (1 x 1 m of cell size). The current scenario (year 2012) was simulated with three flow accumulation algorithms (MD, MD8 and D8). MD8 was linked with the most frequent hydrological response of the sub-catchment (rainfall intensity and stream flow during seven years) and generated the most representative pattern of connectivity, especially in the linear landscape elements (LLE). This algorithm was chosen to simulate the 5 past scenarios (1945, 1956, 1973, 1980 and 2006). In all scenarios the highest connectivity appeared related to trails and roads, as well as to streams and gullies, whereas the lowest appeared related to stonewalls in 1945 and 1956 to hillslopes in 1973, and the following afforestation. Changes in connectivity

mainly depended on the changes in the vegetation factor and in a minor way in the total length, spatial location and type of LLE. Afforestation promoted lower and more stable connectivity at both local and catchment scales.

KEY WORDS: Runoff connectivity; Stream flow; Land abandonment; Afforestation; IC model.

INTRODUCTION

The connectivity concept allows investigating the effect of heterogeneities on the general behavior of a system that contains those heterogeneities and it is an essential factor when modelling dissimilar systems (Antoine et al., 2009). Reaney et al. (2014) related hydrological connectivity to the time required for upslope generated runoff and sediment fluxes to reach an efficient flow channel. According to these authors including Bracken and Croke (2007) runoff connectivity depends on climate, hillslope runoff potential, landscape position, delivery pathway and lateral connectivity. In the last decade, the attention for runoff connectivity increased to serve as a geostatistical tool in hydrology and geomorphology (Parsons et al., 2015) and became a key factor to understand the redistribution dynamics of the soil components in the different compartments of the landscape (Chartin et al., 2013). In this study, we quantified the effects of 70 years of human activities (land abandonment, new infrastructures and afforestation) on runoff connectivity throughout a mountainous sub-catchment in the Central Spanish Pyrenees.

During low intensity rainfall events the kinematic dispersion of runoff is dominant, whereas geomorphologic dispersion becomes more dominant for larger intensities (Rossel et al., 2014). Extreme events activate the entire catchment (Lana-Renault et al., 2014), whereas some parts do not significantly contribute to runoff during low and medium intensity events (López-Vicente et al., 2013a). In Mediterranean and other dryland environments that are characterized by patchy vegetation cover (Foerster et al., 2014), the size, length, spatial distribution and connectivity between the different patches determine the magnitude of the runoff processes (Cammeraat, 2004).

Human organization of landscape elements has a significant control on runoff and soil redistribution processes, so that similar events can produce very different responses (and vice versa) (Lesschen et al., 2009). In the second half of the past century many European and Mediterranean mountainous agricultural landscapes suffered from land abandonment and depopulation, but also were subject to significant afforestation (García-Ruiz and Lana-

Renault, 2011). In the Spanish mountains, afforestation with conifers was used for land reclamation during many years, causing landscape disturbances. The effects at catchment scale were expressed by a clear decrease of connectivity, lower peak flows and runoff and sediment supply to streams (Ortigosa and García-Ruiz, 1995; Sanjuán et al., 2014). Construction of paths, forest roads and firewalls influence runoff connectivity in forested catchments (Croke and Mockler, 2001). Stonewalls and agricultural terraces form an important feature in the Mediterranean landscapes and have an important and clear effect reducing soil loss, runoff coefficients and connectivity (Lesschen et al., 2009; Arnáez et al., 2015). Land abandonment promoted the mismanagement and collapse of these terraces increasing runoff connectivity and soil erosion (López-Vicente et al., 2013b). However, slope terracing without any supporting structure is an aggressive and common man-made technique in afforestation practices (Linares et al., 2002).

In the last decade, several hydrological connectivity indices appeared in the literature, most of them based on Geographic Information System (GIS) and stream-power approaches, such as the "volume to breakthrough" of Bracken and Croke (2007), and the Network Index of Lane et al. (2009). Recently, Reaney et al. (2014) used the Connectivity of Runoff Model, 2D version, in semi-arid environments. A few years ago, Borselli et al. (2008) developed the index of runoff and sediment connectivity (IC) testing successfully this approach in a large catchment in Central Italy against field observations. Afterwards, Cavalli et al. (2013) proposed some improvements on the original equation related to very steep slopes. Gay et al. (2015) executed the index in Central France and improved it for lowlands considering infiltration properties. The ability of the IC model have been proved in different fields and catchments around the World, such as the studies of Heckmann and Schwanghart (2013) in Austria, D'Haen et al. (2013) in Turkey, Vigiak et al. (2012) in Australia, and Chartin et al. (2013) in Japan. In northeastern Spain (López-Vicente et al., 2013b; Foerster et al., 2014) several studies proved its capacity to map runoff and sediment connectivity.

There are no studies dealing with the long-term effects of combined land use changes on runoff connectivity, especially after afforestation practices. Therefore we: (i) evaluated the current conditions (year 2012: no crops, tall pines, three trails, one unpaved forest road and many broken stonewalls) of runoff connectivity using 3 flow accumulation algorithms and the IC model; (ii) analyzed the relationship between each pattern of connectivity and the hydrological response at the sub-catchment outlet (stream flow and rainfall depth) during seven years (October 2007 – September 2014); (iii) simulated the runoff connectivity during five past scenarios (1945, 1956, 1973, 1980 and 2006) with the most appropriate algorithm

and the IC model, and the land use and linear landscape elements (LLE) of each scenario; (iv) evaluated the role of the combined and purely human-induced changes on runoff connectivity for the 6 scenarios; and (v) proposed potential management practices to reduce the negative impacts of high runoff connectivity.

MATERIALS AND METHODS

Study area

The study area corresponds to the afforested sub-catchment of the Araguás catchment (Rebullesa stream) that is located in the Central Spanish Pyrenees near Jaca town (Figure 1A) (42º 36' 15.18'' N; 0º 37' 27.10'' W). The elevation ranges between 899 and 1159 m a.s.l. and the total extension is of 17.2 ha. The landscape is hilly with a minimum and average slope steepness of 4 and 43%, respectively. There is a lack of flat areas and apart from the main gully, that works as the stream, there are several small gullies directly connected to it. In the lower part and near the gauging station badlands are present (Nadal-Romero et al., 2010). The area represented an intensely cultivated landscape until 1950's, which was afforested with coniferous during the 60's and 70's (*Pinus sylvestris* and *Pinus nigra*) (Figure 1B). Modified soils show truncation signs in the surface horizons, low organic matter content and poor structure (Nadal-Romero et al., 2016). The climate is Sub-Mediterranean with Oceanic and Continental influences. Annual rainfall varies between 500 and 1000 mm (average annual rainfall approximately 800 mm), with two major rainfall periods (autumn and spring), convective storms usually occur in summer, and occasional snowfalls in winter (Nadal-Romero et al., 2008).

Land use change and scenarios

A total of 6 aerial photos were used from the digital aerial photo repository of the Spanish National Geographic Institute (http://fototeca.cnig.es/). These photos covered a period of almost 70 years: 1945, 1956, 1973, 1980, 2006 and 2012 (Figure 1C). The four oldest photos had no geometric correction and 15 geographic control points were used to identify the boundary of the sub-catchment. The two more recent images were orthophotos and the complete boundary of the sub-catchment was derived from the digital elevation model (DEM). In the oldest scenario (1945), almost the entire sub-catchment was cultivated with cereals (wheat and barley) and hardly any trees were present and mainly located along the stream. Many stonewalls (ca. 1.2 m height) and terraces controlled the size and shape of the fields and two narrow paths (ca. 1.5 m wide) crossed the hillslope (Table I). In 1956 almost

all fields were continuously cultivated but mismanagement practices of the LLE triggered the breakdown of some of these structures and thus an increment in the number and length of ephemeral gullies. The third scenario (1973), described the early stage (short pines) of the massive coniferous plantation (59% of total surface). Most LLE were still preserved although walls and terraces showed many breaking points. A new narrow trail appeared in the upper part related to the afforestation works. In 1980, the trees were taller and a new unpaved forest road (ca. 3 m wide) appeared. In 2006 the canopy of the pines was well developed and many shrubs covered the abandoned fields and open areas. In the current scenario (2012) (Figure 2A), more sections of terraces and stonewalls were desintegrated due to the long duration of abandonment. The current height of the *P. sylvestris* plantation is ca. 6 m whereas *P. nigra* pines are slightly taller, ca. 6.5 m height (Figure 2B). Some small areas underwent natural plant colonization (secondary succession) with plant species like *Genista scorpius*, *Juniperus communis*, *Rosa gr. canina* and *Buxus sempervirens* (ca. 1 m tall), as well as some stands of young *P. sylvestris*. The different vegetation types appear as heterogeneous patches with many spots of open scrubland and bare soil, with a density of 81.9 patches per hectare.

Field data and monitoring

The sub-catchment is equipped with two tipping buckets that collect rainfall every 5 minutes. At the outlet of the sub-catchment stream flow is measured at a gauging station (V-notch weir) using a water pressure sensor (Keller DCX-22 AA) (Figure 2C). A seven-year record (1 October 2007 – 30 September 2014) of rainfall depth and stream flow were measured and analyzed. We derived a high spatial resolution digital elevation model (DEM) at 1x1 m of cell size from the LiDAR-derived DEM at 5x5 m of cell size, generated by the Spanish National Geographic Institute (IGN; http://centrodedescargas.cnig.es/CentroDescargas/). We selected this spatial resolution to guarantee that the narrow and in some places short LLE were included in the simulation.

The IC model

We used part of the modifications made by Cavalli et al. (2013) on the index of runoff and sediment connectivity (IC) proposed by Borselli et al. (2008). As the study site does not present flat areas we did not consider the modifications made by Gay et al. (2015) for lowlands. The IC model accounts the characteristics of the drainage area (D_{up}, upslope module) and the flow path length that a particle has to travel to arrive at the nearest sink (D_{dn}, downslope module):

$$IC_K = \log_{10}\left(\frac{D_{up,K}}{D_{dn,K}}\right) = \log_{10}\left(\frac{\overline{W_K}\cdot\overline{S_K}\cdot\sqrt{A_K}}{\sum_{i=K,n_K}\frac{d_i}{W_i\cdot S_i}}\right) \quad (1)$$

where $\overline{W}$ is the average weighing factor of the upslope contributing area (dimensionless and equal to the *C-RUSLE* factor), $\overline{S}$ is the average slope gradient of the upslope contributing area (m m^{-1}), A is the upslope contributing area (m^2), d_i is the length of the ith cell along the downslope path (m), W_i is the weight of the ith cell (dimensionless), and S_i is the slope gradient of the ith cell (m m^{-1}). Values of slope steepness lower than 0.005 must be replaced by the value S_i = 0.005 and those higher than 1 must be set to a maximum value of 1. The subscript K indicates that each cell "i" has its own *IC*-value. This index is defined in the range of [−∞, +∞] and connectivity increases when IC grows towards +∞. The role of the linear landscape elements (LLE: agricultural terraces, stonewalls, trails and roads) is added by modifying the original map of flow direction with a mask with two values, 0 for the LLE and 1 for the remaining area.

Connectivity changes due to changes on runoff magnitude, thus we computed different IC maps with three flow accumulation algorithms for the current scenario. We tested the D8 (single direction), MD (multiple direction) and MDD8 (multiple direction with threshold value for linear flow) algorithms (more details in López-Vicente and Navas, 2010; López-Vicente et al., 2014). $\overline{W}$, $\overline{S}$ and A were also calculated with these three algorithms. The "stream mask" was associated with the area where the gully showed a permanent stream (see Appendix A in Borselli et al., 2008). We used the values of the *C-RUSLE* factor obtained by López-Vicente and Navas (2009) and López-Vicente et al. (2011) in two catchments of the Pyrenees with similar vegetation as that of the study area. For badlands and gullies we used the value proposed by Capolongo et al. (2008) in a semiarid area in Southern Italy. For the low (early stage of plantation), mid and high (current scenario) elevation pine forest we used the values proposed by De Tar et al. (1980) and Miller et al. (2003).

RESULTS

Current scenario of stream flow and runoff connectivity

The average annual rainfall (R) and stream flow (Q) during the 7 hydrological years were 783 and 244 mm year^{-1} (Figure 3A), obtaining an average runoff coefficient of 31%. A total of 1339 rainfall events (e) were recorded and only 13% of these events (n=168) were considered

as erosive events (*ee*) (Figure 3B). According to Renard et al. (1997), an erosive event had a total rainfall depth equal or higher than 12.7 mm, or lower than 12.7 mm but with a minimum maximum rainfall intensity of 6.35 mm in 15 minutes. Values of *R*, *Q* and maximum rainfall intensity during all events (I_{30}-*e*) including the erosive events (I_{30}-*ee*), showed a marked variability (Figure 3C). The mean values of *R*, *Q*, I_{30}-*e* and I_{30}-*ee* were of 61.8 and 19.8 mm month^{-1} and 3.1 and 10.2 mm h^{-1}, respectively, and their coefficients of variation were 0.7, 1.3, 1.0 and 1.1. Values of daily rainfall did not correlate well with those of stream flow (r = 0.237). Thus, we selected the monthly values of *Q* and I_{30}-*ee* to describe and identify three different hydrological periods (HyP). The HyP1 from January to March when the highest values of *Q* (ca. 41.2 mm month^{-1}) were registered, and August when the highest values of I_{30}-*ee* (ca. 29.2 mm h^{-1}) appeared. This period represented the most intense hydrological response of the sub-catchment. The HyP2 had the longest period (6 months), from April to July and from September to October, when moderate values of *Q* and I_{30}-*ee* were registered, and it represented the most predominant conditions. The short HyP3, from November to December, represented the period with the lowest activity, when the lowest values of *Q* (ca. 8.4 mm month^{-1}) and I_{30}-*ee* (ca. 4.4 mm h^{-1}) were observed (Figure 3D).

In the current scenario, the total length of the LLE was 3073 m and the *C-RUSLE* factor had a mean value of 0.0836 (Figure 4) (Table I). The IC map obtained with the MD algorithm represented dispersed overland flow patterns without presence or limited occurrence of concentrated runoff (Figure 5A). The IC map with the MD8 algorithm represented the occurrence of concentrated runoff from a threshold value downwards and disperse flow near the divides (Figure 5B). The threshold value was associated with the initiation of the gullies and the permanent rills of the ruined terraces. The IC map with the D8 algorithm represented very concentrated overland flow from divides to the stream (Figure 5C). Each map showed a different mean value and range due to the specific characteristics of each algorithm. Because the different values of rainfall intensity and depth trigger different patterns of runoff, we linked the IC-MD map with the HyP3 period, the IC-MD8 map with HyP2, and the IC-D8 map with HyP1. The frequency histograms of the three maps of connectivity showed a similar pattern although the histogram of the MD8 approach was the closest to a normal distribution (Figure 5D). Finally, the MD8 algorithm was the most appropriate to describe the average spatial pattern and variability of runoff connectivity and thus we ran the IC model with this algorithm in the 5 past scenarios.

The highest values of connectivity appeared on the road and trails, followed by stonewalls and terraces, and in the stream and gullies (Table II). Lower values of connectivity appeared

upslope the forest road comparing to downslope, highlighting the key role of this infrastructure on the magnitude of connectivity throughout the hillslopes. The afforested areas presented the lowest values of connectivity due to the protective effect of the pine plantation, as reflected in the low values of the *C-RUSLE* factor of both pine species.

Runoff connectivity during the past scenarios

Values and spatial patterns of connectivity clearly changed in the five past scenarios in comparison with the current situation (Figure 6, Table III). The analysis was done from the most recent past scenario to the oldest. In 2006 the total length of the LLE was slightly longer and differences in vegetation were small (Figure 4) (Table I). The mean connectivity in 2006 was the lowest of the six scenarios although it was very similar to that in 2012 (Figure 6E). In 1980, the total length of the LLE was 4% longer than the total current length though the mean connectivity was 19% higher due to the small/medium size of the pine plantation (Figure 6D). The abandonment of an old trail and the creation of a new one located upslope, modified the spatial patterns and values of connectivity in 2006 in comparison to 1980. In 1973, the total length of the LLE was quite similar to that in 1980, although in 1973 the forest road that controlled the spatial patterns of connectivity did not yet exist in 1980 and in later scenarios. Hence, the changes in connectivity in 1980 in comparison with 1973 were explained by both the changes in the *C-RUSLE* factor and the spatial location of the LLE (Figure 6C and 7A).

In 1956 and 1945, the lengths of the LLE were, respectively, 40 and 70% longer than in 2012 (Figure 4) and the land use maps were clearly different, with many cereal fields. Hence, the maps of connectivity in 1945 and 1956 showed different spatial patterns and the highest values of connectivity of the six scenarios (Figure 6A and 6B). The collapse of some sections of stonewalls in 1956 and the main land use (crop) resulted in the highest values of connectivity in that year. The mean connectivity in 1945 was 42% higher than in 2012 and conversely connectivity in 2012 was 82% lower than in 1945 (Figures 6A and F). Surfaces that currently present higher values of connectivity only affected 6% of the total surface and were associated with a forest road, a new trail, some sections of stonewalls, abandoned fields and small areas near the stream and bare lands. Areas showing a decrease in connectivity were predominant and affected 94% of the surface. During the six scenarios the highest values of connectivity appeared on the trails and road, followed by stream and gullies, whereas the lowest values appeared in stonewalls and terraces in 1945 and 1956, and for the hillslopes in 1973 and the following scenarios due to the afforestation (Table III).

The density of LLE also modified the mean and maximum length of the flow path lines (FPL) in each scenario (Table III). The 1945 presented the shortest mean value of the FPL due to the highest density of LLE in the study area. This value increased in 1956 and reached the longest value in 1973 due to the tumble down of many sections of the stonewalls. The construction of the forest road reduced the mean and maximum length of the FPL in 1980 and next scenarios. The beginning of afforestation in 1973 slightly reduced the maximum length of FPL. The variability of the IC values at short distance, estimated by analyzing the values of the eight surrounding pixels of each pixel, also changed during the 6 scenarios (Table III). The highest local variability appeared in 1945 and 1956, whereas the most stable local patterns appeared in 2012. Hence, afforestation promoted lower and more stable values of runoff connectivity.

DISCUSSION

The different patterns and values of connectivity that we found for the Araguás sub-catchment throughout the year, were also revealed by Zimmermann et al. (2014) at monthly resolution, and in the forests of the Panama Canal Watershed, supporting the importance of selecting an adequate spatial approach to study overland flow patterns. Foerster et al. (2014) also found different connectivity maps for contrasting seasons in a 70 km^2 catchment in the Spanish Pyrenees. They obtained the highest connectivity values in August comparable to what we described in the IC-D8 map for HyP1. Few evaluations of the hydrological effects of afforestation in humid Mediterranean areas have been carried out at catchment scale, stressing the lack of available information. Nadal-Romero et al. (2016) showed that seasonal differences in hydrological response and connectivity exist in the same afforested sub-catchment we were studying, and they suggested different runoff generation processes: an alternation between a wet period, when the catchment was hydrologically responsive, and a dry summer period when the catchment was not or rarely responsive, and two transitional periods. This pattern is partially coherent with the analyses presented here. The HyP1 from January to March coincides with the wet period and the most intense hydrological response, including August resulting from high rainfall intensities. The HyP2 (from April to July and from September to October) could correspond to the two transitional periods. According to Nadal-Romero et al. (2016), the HyP3 wouldn´t correspond with summer. This time gap could be due to the frequent occurrence of intense rainstorms during the summer period demonstrating a lower efficiency to reduce flooding risk after afforestation programs. In a neighboring catchment, the Arnás river catchment (abandoned fields with natural

revegetation), three periods were identified by Lana-Renault et al. (2007): i) the wet period, from the beginning of December to the middle of May (linked with the HyP1); ii) the drying-up period, from May-June to the end of the summer season (similar to our HyP2); and iii) the wetting-up period, that started with the first autumn rainfall events and lasts until the end of November (or later) and that could be associated to the HyP3.

The high values of connectivity in the two oldest scenarios and the marked decrease in connectivity after land abandonment and afforestation agreed with the results of connectivity, runoff and sediment yield dynamics reported by Sanjuán et al. (2014) and Buendia et al. (2016) in the Spanish Pyrenees and Pre-Pyrenees, which were linked to land cover changes and afforestation, respectively. Hawtree et al. (2015) also found in a large and wet catchment in North-Central Portugal that pine afforestation promoted slower flow pathways, especially during the wet season, by increasing the amount of water entering the soil matrix via infiltration due to the ground preparation and planting operations used. However, these authors also described a faster catchment response with young eucalypt and older pine plantations, possibly due to soil water repellency. Baartman et al. (2013) obtained with both virtual and real catchments that connectivity decreased with increasing landscape morphological complexity. We also observed this association in the Araguás sub-catchment between: i) the complex patterns of patched vegetation in 2006 and 2012, and the low values of connectivity; and ii) the simple land uses in 1945 and 1956, and the highest values of connectivity.

Changes in the total length and position of the LLE and those of the vegetation (*C-RUSLE* factor) played a different role in the evolution of the simulated values of runoff connectivity in the six scenarios (Table III). These results agreed with those obtained by Marchamalo et al. (2015) in a semi-arid environment where man-made lines (terraces and tracks) and the presence of vegetation influenced differently the local and catchment values of sediment connectivity. On the basis on 2012, when vegetation hardly changed, as was also the case in 2006 (C-RUSLE 0.4% higher), the small increment of the total length of the LLE (1.6%) explained the slight decrease in connectivity (-1.4%). However, when both factors changed, such as in 1980, the role played by vegetation changes (C-RUSLE 33.8% higher) was more important than the increment of the total length of the LLE (3.9%), and thus the runoff connectivity clearly increased (19.3%) (Figure 7A). In order to estimate the specific contribution of the changes in the LLE and the vegetation cover to the total change of connectivity in each scenario, we ran the IC model in the 5 past scenarios only considering

changes in the LLE (fixed map of *C-RUSLE*). Then, we ran the IC model considering that changes only happen in the vegetation cover (fixed map of LLE). When only LLE changed the values of runoff connectivity varied between -1.7 and 5.7%, whereas the range of changes triggered by vegetation changes was between 0.05 and 41.3% (Figure 7B).

In spite of the positive effects of afforestation reducing runoff connectivity, the mean length of the FPL increased due to the loss of stonewalls. This fact could explain the similar and very high values of connectivity as reported by Lana-Renault et al. (2014) in other comparable areas in the Pyrenees during high intensity summer rainstorms, when entire catchments were activated. Monitoring of the changes in LLE, vegetation growth and stream flow are included in current and future research planning. We also plan to run the spatially-distributed hydrological DR2 model (López-Vicente et al., 2014) to make a stronger analysis of the hydrological response of the soils. In order to reduce the negative impacts of high runoff connectivity of gullies and degraded (bare soil and open scrubland) areas on the Araguás sub-catchment, we propose to rebuild some of the destructed stonewalls. This practice should focus on those areas where the length of the FPL reaches higher values. Twenty years ago, Gallart et al. (1994) highlighted in a small catchment in the Eastern Pyrenees the environmental hazard of the spontaneous reorganization of the unmaintained artificial drainage network of abandoned terraces. Zimmermann et al. (2014) showed that the length of the FPL and its location is crucial to understand the magnitude of runoff connectivity. The recovery of stonewalls can be also considered as a structural measure to prevent off-site effects of soil erosion and corresponds well with the suggestions recently proposed by Mekonnen et al. (2015) on soil conservation through sediment trapping. Knowledge of the spatial pattern of connectivity and its dynamics over time is essential for land and water resource management, and for understanding the potential environmental effects of land use changes. Research on hydrological connectivity can also help to increase the understanding of the effects of afforestation, land abandonment, timberland, skid trails, and other forest practices in mountain landscapes and thus can provide crucial knowledge to land managers, policy makers and stakeholders.

CONCLUSIONS

In the current scenario, the combined analysis of the spatially distributed values of runoff connectivity and the temporal changes in the hydrological response of the sub-catchment

improved our ability to understand the complexity of water dynamics. The multiple flow algorithm with threshold value for linear flow (MD8) generated the most representative map in the current scenario, and thus, it was selected to run the index of connectivity for the past scenarios. The observed changes in connectivity mainly depended on the changes in the vegetation factor (C-RUSLE) and in a minor way on the total length, spatial location and type of the linear landscape elements. However, when small vegetation differences occurred the role of the changes in the LLE became more important than the changes in the vegetation. Afforestation promoted lower and more stable values of runoff connectivity reducing the local variability of the values of runoff connectivity. However, the collapse of many sections of stonewalls and terraces favored the increment of the mean length of the flow path lines (FPL). We propose to rebuild the ruined stonewalls in those areas where the length of the FPL reached a high value to avoid significant increases of runoff connectivity especially during intense summer storm events. These results and the conservation proposal can be of interest for hydrological and forestry projects both for the public and private sectors.

ACKNOWLEDGEMENTS

This research was supported by a Marie Curie Intra-European Fellowship in the project "MED-AFFOREST" (PIEF-GA-2013-624974). Dr. López-Vicente acknowledges the financial support of his postdoctoral contract to the project "EroCostModel" (CGL2014-54877-JIN; Programme *Jóvenes Investigadores*) and Dr. Nadal-Romero was recipient of a *Ramón y Cajal* research contract. Both contracts are of the Spanish Ministry of Economy and Competitiveness.

REFERENCES

Antoine M, Javaux M, Bielders C. 2009. What indicators can capture runoff-relevant connectivity properties of the micro-topography at the plot scale? *Advances in Water Resources* **32**(8): 1297–1310. DOI: 10.1016/j.advwatres.2009.05.006.

Arnáez J, Lana-Renault N, Lasanta T, Ruiz-Flaño P, Castroviejo J. 2015. Effects of farming terraces on hydrological and geomorphological processes. A review. *Catena* **128**: 122–134. DOI: 10.1016/j.catena.2015.01.021.

Baartman JEM, Masselink R, Keesstra SD, Temme AJAM. 2013. Linking landscape morphological complexity and sediment connectivity. *Earth Surface Processes and Landforms* **38**(12): 1457–1471. DOI: 10.1002/esp.3434.

Borselli L, Cassi P, Torri D. 2008. Prolegomena to sediment and flow connectivity in the landscape: A GIS and field numerical assessment. *Catena* **75**(3): 268–277. DOI: 10.1016/j.catena.2008.07.006.

Bracken LJ, Croke J. 2007. The concept of hydrological connectivity and its contribution to understanding runoff-dominated geomorphic systems. *Hydrological Processes* **21**(13): 1749–1763. DOI: 10.1002/hyp.6313.

Buendia C, Bussi G, Tuset J, Vericat D, Sabater S, Palau A, Batalla RJ. 2016. Effects of afforestation on runoff and sediment load in an upland Mediterranean catchment. *Science of the Total Environment* **540**: 144–157. DOI: 10.1016/j.scitotenv.2015.07.005.

Cammeraat ELH. 2004. Scale dependent thresholds in hydrological and erosion response of a semi-arid catchment in southeast Spain. *Agriculture, Ecosystems and Environment* **104**: 317–332. DOI: 10.1016/j.agee.2004.01.032.

Capolongo D, Pennetta L, Piccarreta M, Fallacara G, Boenzi F. 2008. Spatial and temporal variations in soil erosion and deposition due to land-levelling in a semi-arid area of Basilicata (Southern Italy). *Earth Surface Processes and Landforms* **33**(3): 364 –379. DOI: 10.1002/esp.1560.

Cavalli M, Trevisani S, Comiti F, Marchi L. 2013. Geomorphometric assessment of spatial sediment connectivity in small Alpine catchments. *Geomorphology* **188**: 31–41. DOI: 10.1016/j.geomorph.2012.05.007.

Chartin C, Evrard O, Onda Y, Patin J, Lefèvre I, Ottlé C, Ayrault S, Lepage H, Bonte P. 2013. Tracking the early dispersion of contaminated sediment along rivers draining the Fukushima radioactive pollution plume. *Anthropocene* **1**: 23–34. DOI: 10.1016/j.ancene.2013.07.001.

Croke J, Mockler S. 2001. Gully initiation and road-to-stream linkage in a forested catchment, southeastern Australia. *Earth Surface Processes and Landforms* **26**(2): 205–217. DOI: 10.1002/1096-9837(200102)26:2<205::AID-ESP168>3.0.CO;2-G.

De Tar WR, Ross JJ, Cunningham RL. 1980. Estimating the C factor in the Universal Soil Loss Equation for landscape slopes. *J. Soil & Water Cons.* **35**(1): 40–41.

D'Haen K, Dusar B, Verstraeten G, Degryse P, De Brue H. 2013. A sediment fingerprinting approach to understand the geomorphic coupling in an eastern Mediterranean mountainous river catchment. *Geomorphology* **197**: 64–75. DOI: 10.1016/j.geomorph.2013.04.038.

Foerster S, Wilczok C, Brosinsky A, Segl K. 2014. Assessment of sediment connectivity from vegetation cover and topography using remotely sensed data in a dryland catchment in the Spanish Pyrenees. *Journal of Soils and Sediments* **14**: 1982–2000. DOI: 10.1007/s11368-014-0992-3.

Gallart F, Llorens P, Latron J. 1994. Studying the role of old agricultural terraces on runoff generation in a small Mediterranean mountainous basin. *Journal of Hydrology* **159**: 291–303. DOI: 10.1016/0022-1694(94)90262-3.

García-Ruiz JM, Lana-Renault N. 2011. Hydrological and erosive consequences of farmland abandonment in Europe, with special reference to the Mediterranean region – A review. *Agriculture, Ecosystems and Environment* **140**: 317–338. DOI: 10.1016/j.agee.2011.01.003.

Gay A, Cerdan O, Mardhel V, Desmet M. 2015. Application of an index of sediment connectivity in a lowland area. *Journal of Soils and Sediments*: DOI 10.1007/s11368-015-1235-y.

Hawtree D, Nunes JP, Keizer JJ, Jacinto R, Santos J, Rial-Rivas ME, Boulet A-K, Tavares-Wahren F, Feger K-H. 2015. Time series analysis of the long-term hydrologic impacts of afforestation in the Águeda watershed

of north-central Portugal. *Hydrology and Earth System Sciences* **19**: 3033–3045. DOI: 10.5194/hess-19-3033-2015.

Heckmann T, Schwanghart W. 2013. Geomorphic coupling and sediment connectivity in an alpine catchment - Exploring sediment cascades using graph theory. *Geomorphology* **182**: 89–103. DOI: 10.1016/j.geomorph.2012.10.033.

Lana-Renault N, Latron J, Regüés D. 2007. Streamflow response and water-table dynamics in a sub-Mediterranean research catchment (Central Pyrenees). *Journal of Hydrology* **347**(3-4): 497-507. DOI: 10.1016/j.jhydrol.2007.09.037.

Lana-Renault N, Nadal-Romero E, Serrano-Muela MP, Alvera B, Sánchez-Navarrete P, Sanjuan Y, García-Ruiz JM. 2014. Comparative analysis of the response of various land covers to an exceptional rainfall event in the central Spanish Pyrenees, October 2012. *Earth Surface Processes and Landforms* **39**(5): 581–592. DOI: 10.1002/esp.3465.

Lane SN, Reaney SM, Heathwaite AL. 2009. Representation of landscape hydrological connectivity using a topographically driven surface flow index. *Water Resources Research* **45**(8): W08423. DOI: 10.1029/2008WR007336.

Lesschen JP, Schoorl JM, Cammeraat ELH. 2009. Modelling runoff and erosion for a semi-arid catchment using a multi-scale approach based on hydrological connectivity. *Geomorphology* **109**(3-4): 174–183. DOI: 10.1016/j.geomorph.2009.02.030.

Linares R, Rosell J, Palli L, Roque C. 2002. Afforestation by slope terracing accelerates erosion. A case study in the Barranco de Barcedana (Conca de Tremp, NE Spain). *Environmental Geology* **42**(1): 11–18. DOI: 10.1007/s00254-002-0527-x.

López-Vicente M, Lana-Renault N, García-Ruiz JM, Navas A. 2011. Assessing the potential effect of different land cover management practices on sediment yield from an abandoned farmland catchment in the Spanish Pyrenees. *Journal of Soils and Sediments* **11**(8): 1440–1455. DOI: 10.1007/s11368-011-0428-2.

López-Vicente M, Navas A. 2009. Predicting soil erosion with RUSLE in Mediterranean agricultural systems at catchment scale. *Soil Science* **174**(5): 272-282. DOI: 10.1097/SS.0b013e3181a4bf50.

López-Vicente M, Navas A. 2010. Routing runoff and soil particles in a distributed model with GIS: implications for soil protection in mountain agricultural landscapes. *Land Degradation & Development* **21**(2): 100–109. DOI: 10.1002/ldr.901.

López-Vicente M, Navas A, Gaspar L, Machín J. 2013a. Advanced modelling of runoff and soil redistribution for agricultural systems: the SERT model. *Agricultural Water Management* **125**: 1–12. DOI: 10.1016/j.agwat.2013.04.002.

López-Vicente M, Pérez-Bielsa C, López-Montero T, Lambán LJ, Navas A. 2014. Runoff simulation with eight different flow accumulation algorithms: Recommendations using a spatially distributed and open-source model. *Environmental Modelling & Software* **62**: 11–21. DOI: 10.1016/j.envsoft.2014.08.025.

López-Vicente M, Poesen J, Navas A, Gaspar L. 2013b. Predicting runoff and sediment connectivity and soil erosion by water for different land use scenarios in the Spanish Pre-Pyrenees. *Catena* **102**: 62–73. DOI: 10.1016/j.catena.2011.01.001.

Marchamalo M, Hooke JM, Sandercock PJ. 2015. Flow and Sediment Connectivity in Semi-Arid Landscapes in SE Spain: Patterns and Controls. *Land Degradation and Development*: DOI: 10. 1002/ldr. 2352.

Mekonnen M, Keesstra SD, Stroosnijder L, Baartman JEM, Maroulis J. 2015. Soil conservation through sediment trapping: A review. *Land Degradation & Development* **26**(6): 544–556. DOI: 10.1002/ldr.2308.

Miller JD, Nyhan JW, Yool SR. 2003. Modeling potential erosion due to the Cerro Grande Fire with a GIS-based implementation of the Revised Universal Soil Loss Equation. *Int. J. Wildland Fire* **12**: 85–100. DOI: 10.1071/WF02017.

Nadal-Romero E, Cammeraat E, Serrano P, Lana-Renault N, Regüés D. 2016. Hydrological response of an afforested catchment in a Mediterranean humid mountain area: a comparative study with a natural forest. *Hydrological Processes*: DOI: 10.1002/hyp.10820.

Nadal-Romero E, Regüés D, Latron J. 2008. Relationships among rainfall, runoff, and suspended sediment in a small catchment with badlands. *Catena* **74**(2): 127–136. DOI: 10.1016/j.catena.2008.03.014.

Nadal-Romero E, Regüés D, Serrano-Muela P. 2010. Respuesta hidrológica en una pequeña cuenca experimental pirenaica con dos ambientes extremos: cárcavas y bosque de repoblación. *Pirineos* **165**: 135-155. DOI: 10.3989/Pirineos.2010.165007.

Ortigosa L, García-Ruiz JM. 1995. Geomorphological consequences of afforestation at a basin scale, an example from the Central Pyrenees. *Physics and Chemistry of the Earth* **20**(3-4): 345–349. DOI: 10.1016/0079-1946(95)00047-X.

Parsons AJ, Bracken L, Poeppl RE, Wainwright J, Keesstra SD. 2015. Introduction to special issue on connectivity in water and sediment dynamics. *Earth Surface Processes and Landforms* **40**(9): 1275–1277. DOI: 10.1002/esp.3714.

Reaney SM, Bracken LJ, Kirkby MJ. 2014. The importance of surface controls on overland flow connectivity in semi-arid environments: Results from a numerical experimental approach. *Hydrological Processes* **28**(4): 2116–2128. DOI: 10.1002/hyp.9769.

Renard KG, Foster GR, Weesies GA, McCool DK, Yoder DC. 1997. Predicting Soil Erosion by Water: A Guide to Conservation Planning with the Revised Universal Soil Loss Equation (RUSLE). Handbook #703. US Department of Agriculture, Washington, DC.

Rossel F, Gironás J, Mejía A, Rinaldo A, Rodriguez F. 2014. Spatial characterization of catchment dispersion mechanisms in an urban context. *Advances in Water Resources* **74**: 290–301. DOI: 10.1016/j.advwatres.2014.09.005.

Sanjuán Y, Gómez-Villar A, Nadal-Romero E, Álvarez-Martínez J, Arnáez J, Serrano-Muela MP, Rubiales JM, González-Sampériz P, García-Ruiz JM. 2014. Linking land cover changes in the sub-alpine and montane belts to changes in a torrential river. *Land Degradation and Development*: DOI: 10.1002/ldr.2294.

Vigiak O, Borselli L, Newham LTH, McInnes J, Roberts AM. 2012. Comparison of conceptual landscape metrics to define hillslope-scale sediment delivery ratio. *Geomorphology* **138**: 74–88. DOI: 10.1016/j.geomorph.2011.08.026.

Zimmermann B, Zimmermann A, Turner BL, Francke T, Elsenbeer H. 2014. Connectivity of overland flow by drainage network expansion in a rain forest catchment. *Water Resources Research* **50**(2): 1457–1473. DOI: 10.1002/2012WR012660.

Figure 1. Location of the Araguás catchment within the Aragón catchment in NE Spain (Central Pyrenees) (A). Images of the pine forest plantation on terraces and a forest road (B). Old aerial photos and recent orthophotos of the study area over 6 different years in a 70-year-period (C).

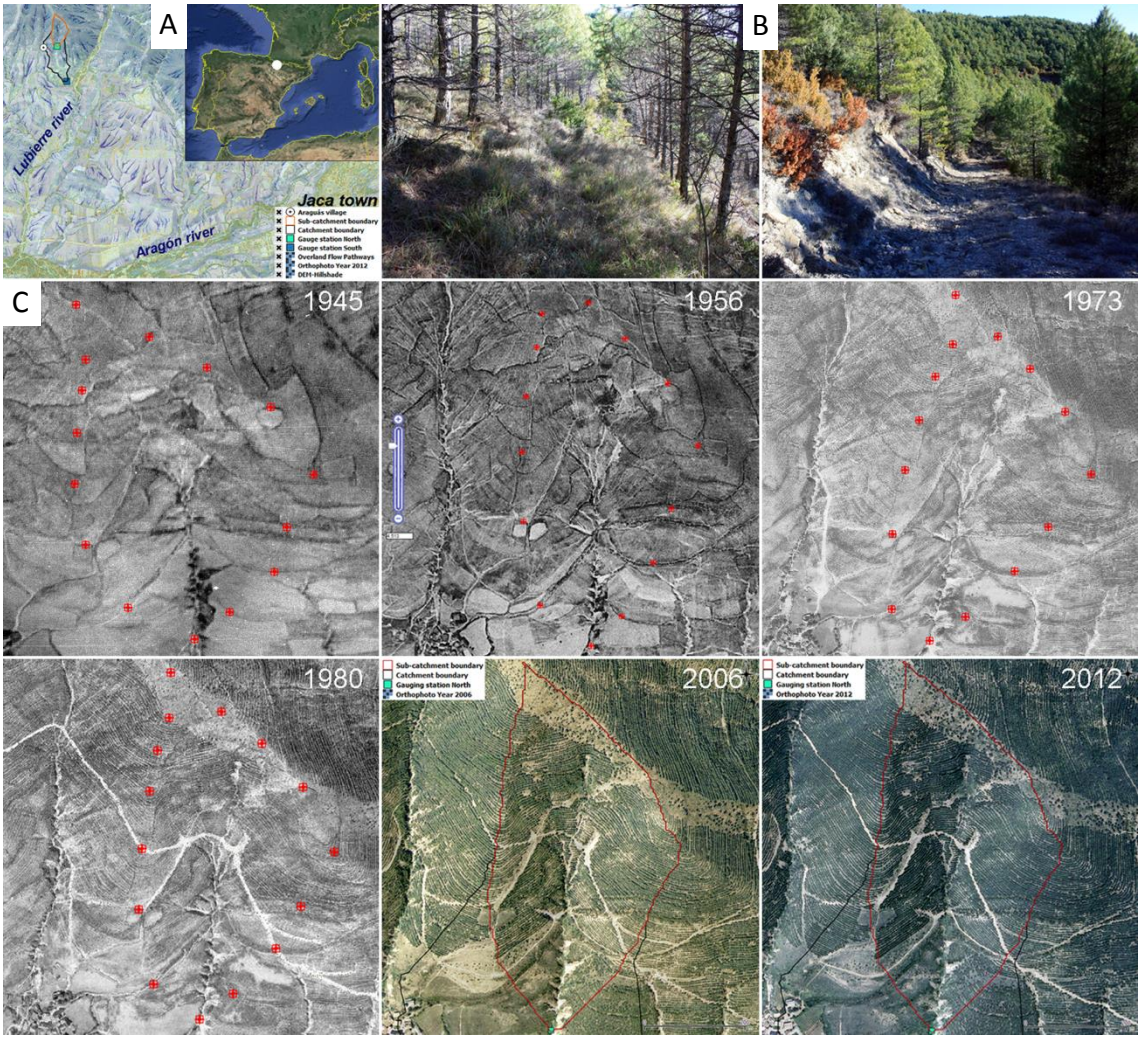

Figure 2. Map of current land use in the afforested Araguás sub-catchment (A). Images of stonewalls and trails in the study area (B) and of the gauging station at the outlet (C).

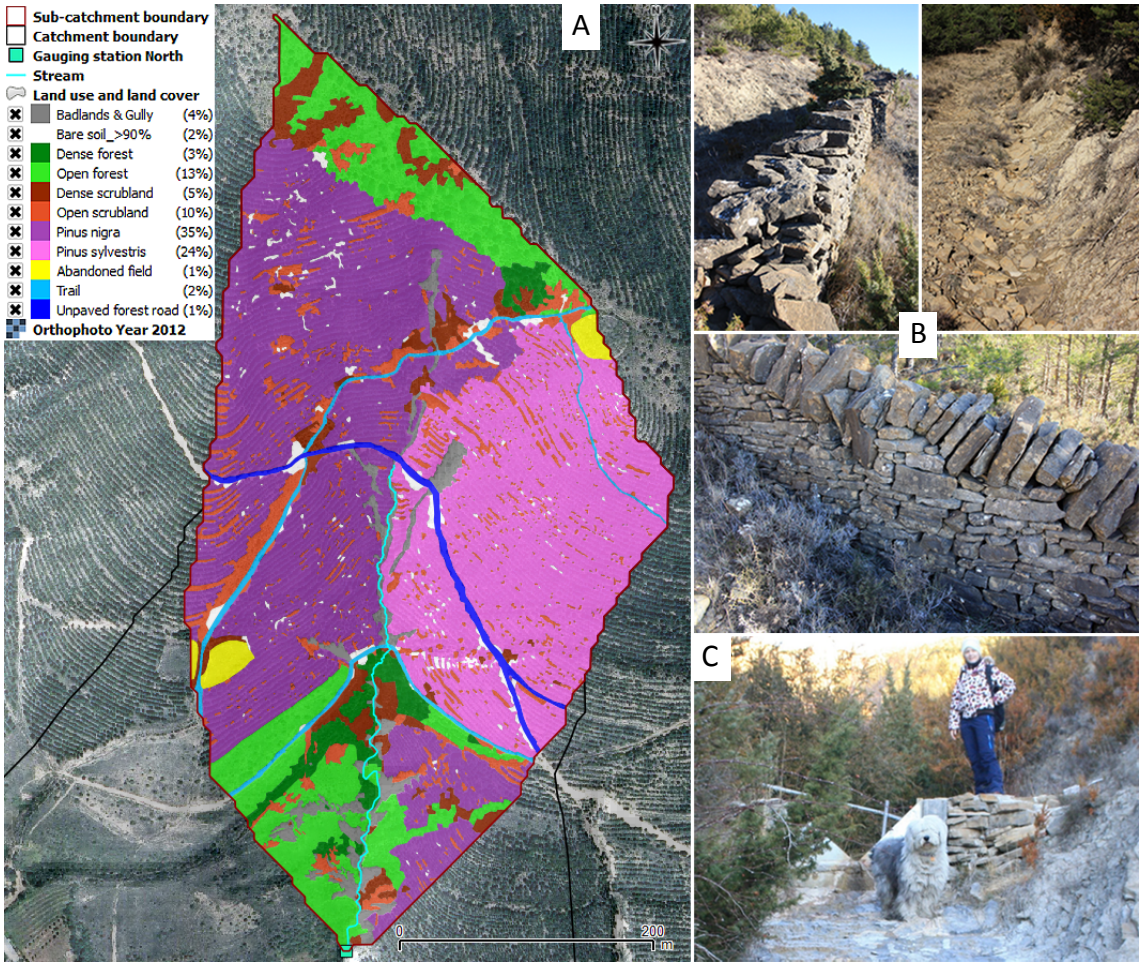

Figure 3. Daily rainfall (*R*) and stream flow (*Q*) depth during the study period (A). Monthly number of rainfall and erosive rainfall events (B) and of the maximum rainfall intensity during all the rainfall events (I_{30}-*e*) and the erosive events (I_{30}-*ee*) (C). Average monthly values of *R*, *Q*, I_{30}-*e*, I_{30}-*ee* and percentage of erosive events (*ee*) (D).

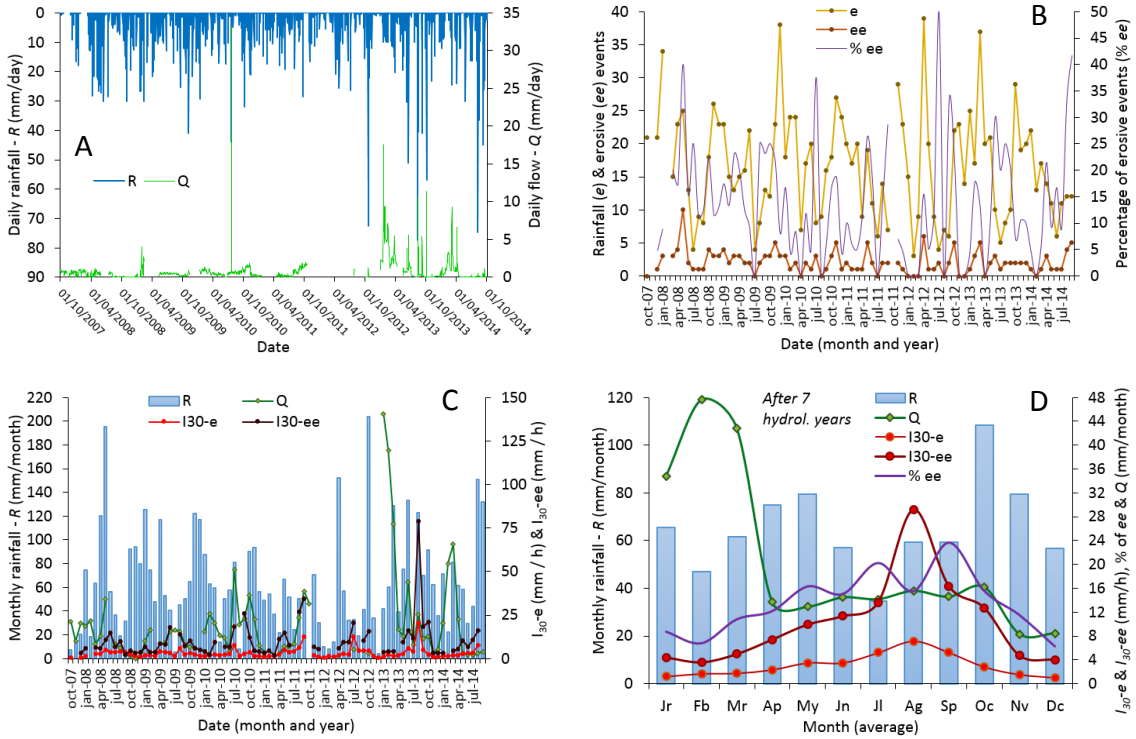

Figure 4. Maps of linear landscape elements (LLE) for the six simulated scenarios.

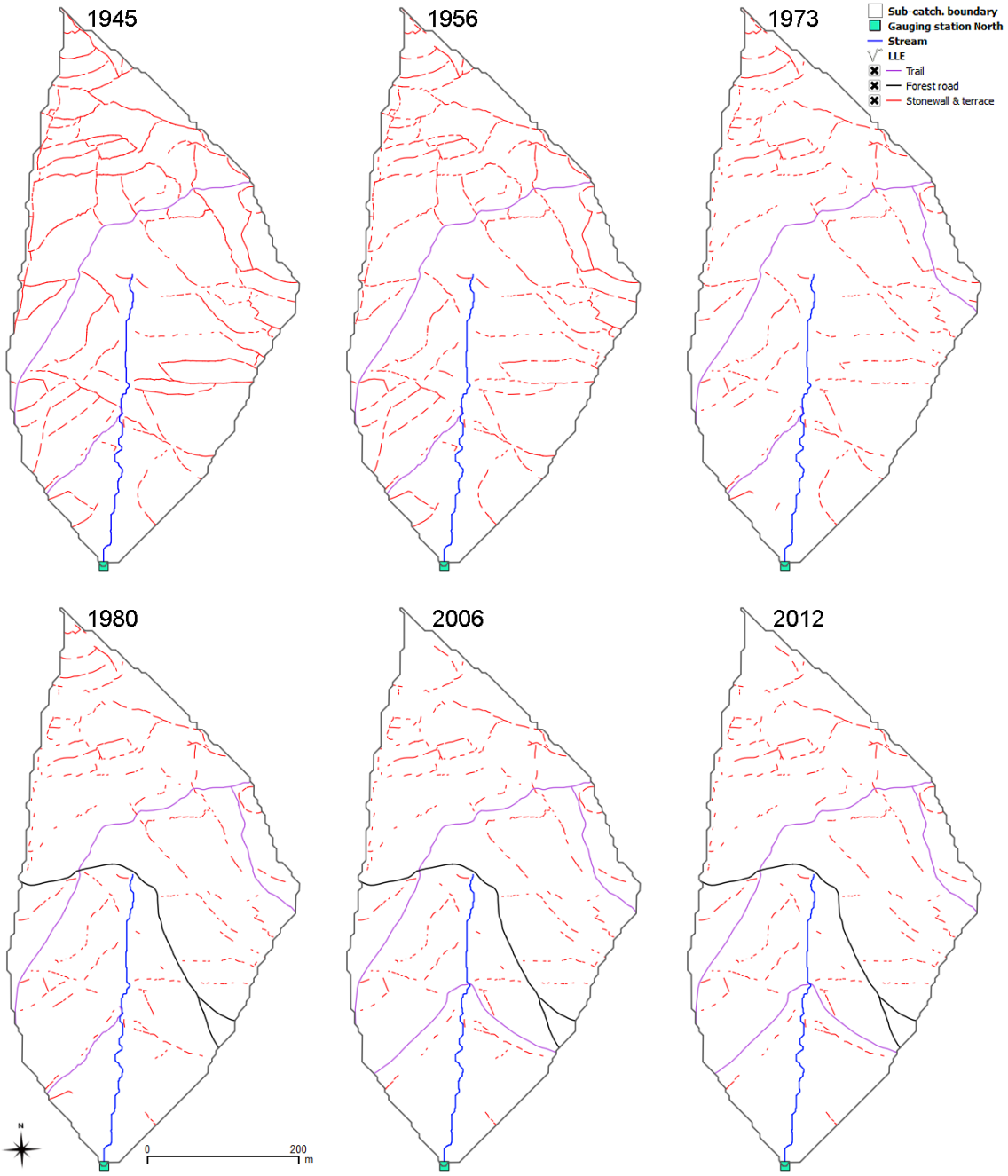

Figure 5. Maps of runoff connectivity calculated with the MD (A), MD8 (B) and D8 (C) algorithms. Frequency histograms of the values of runoff connectivity for each map (D).

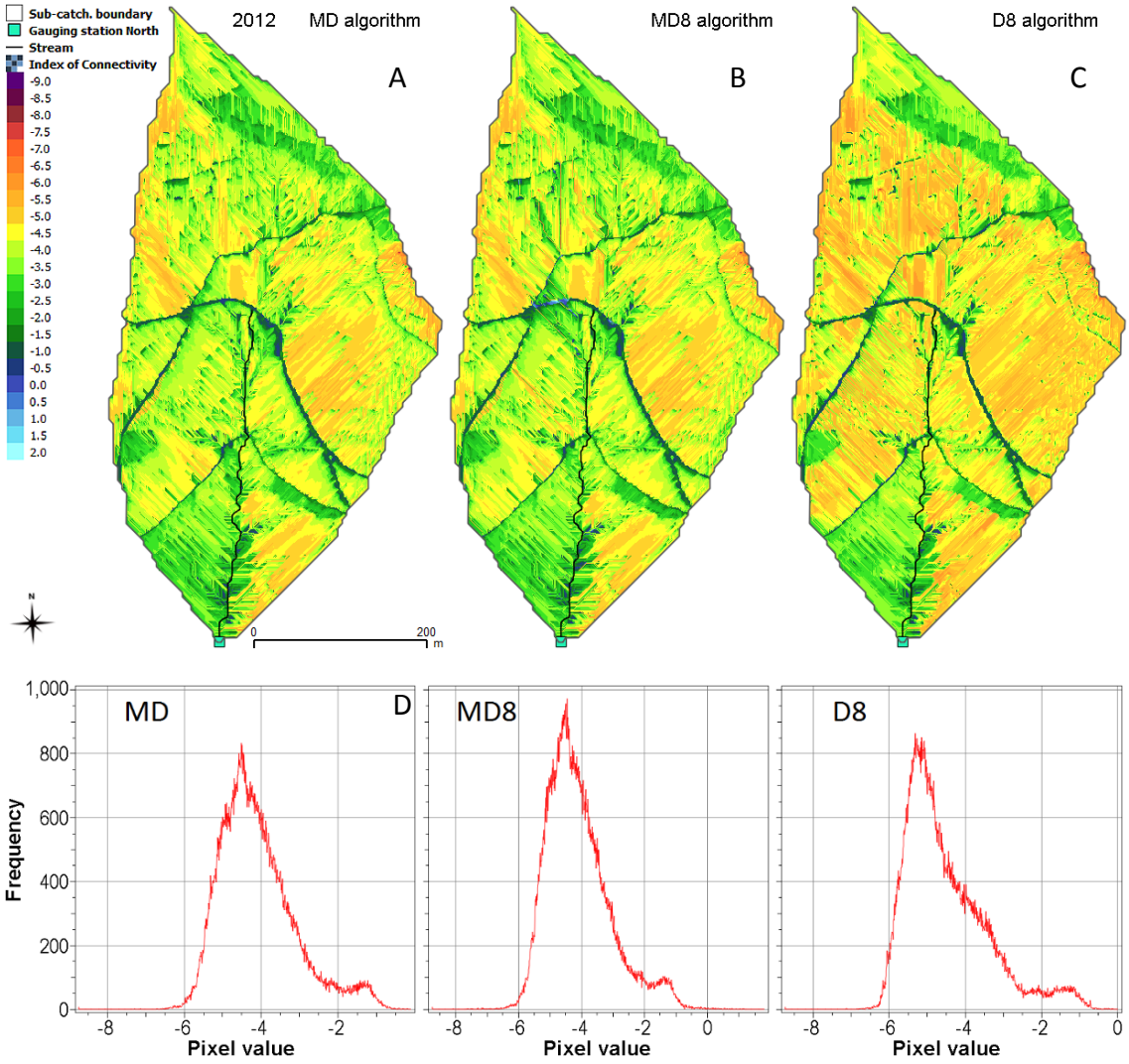

Figure 6. Maps of runoff connectivity in the 5 oldest scenarios (A, B, C, D and E) and of the differences in runoff connectivity between the most recent scenario (2012) and the oldest (1945) (F).

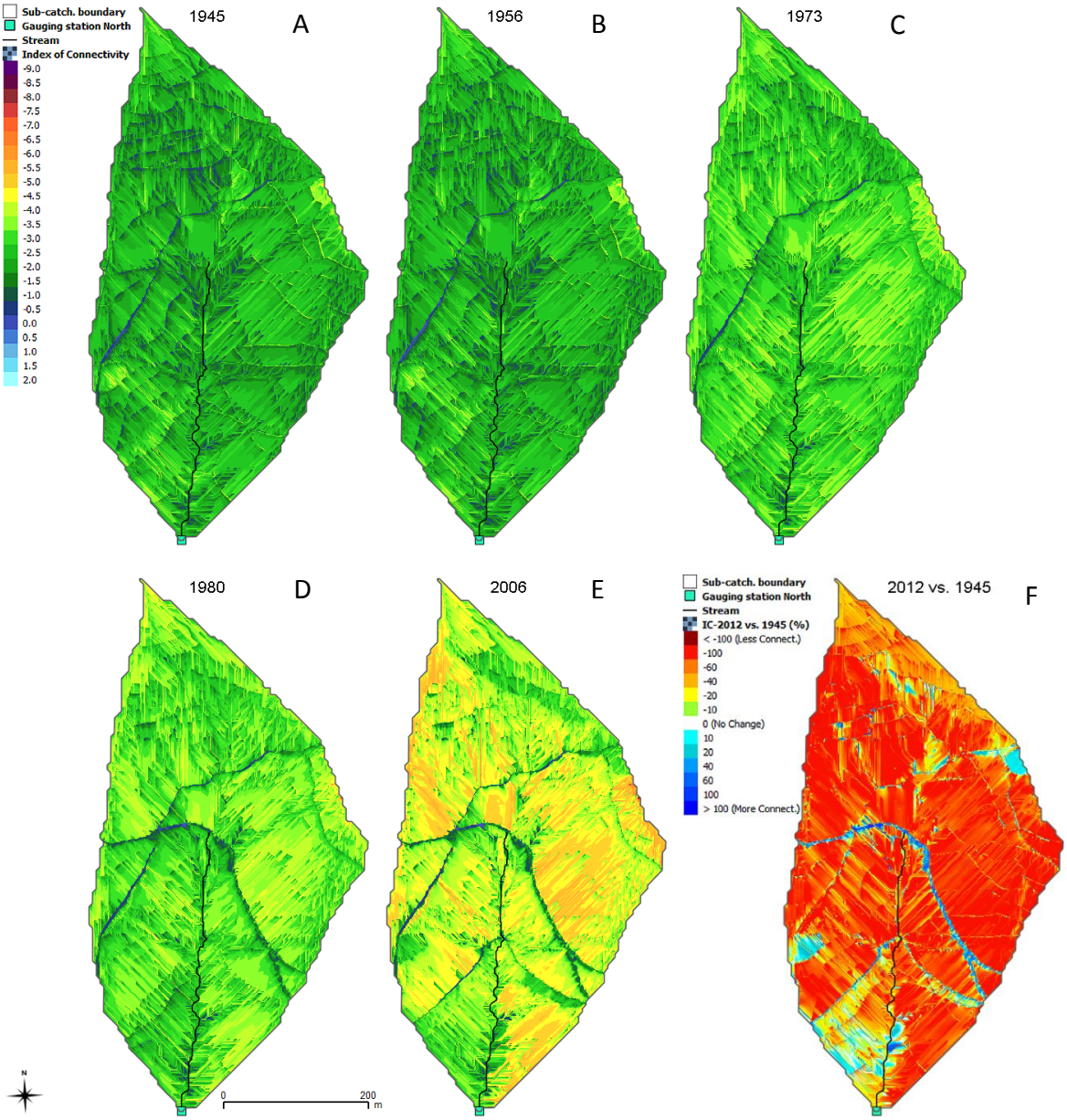

Figure 7. Relative changes in the values of overland flow connectivity (IC), total length of the landscape linear elements (LLE) and the C-RUSLE factor during the 5 past scenarios in comparison with the current scenario (year 2012) (A). Specific contribution played by the alone changes in the LLE and the C-RUSLE factor on the IC value for each past scenario in comparison with the current scenario (B).

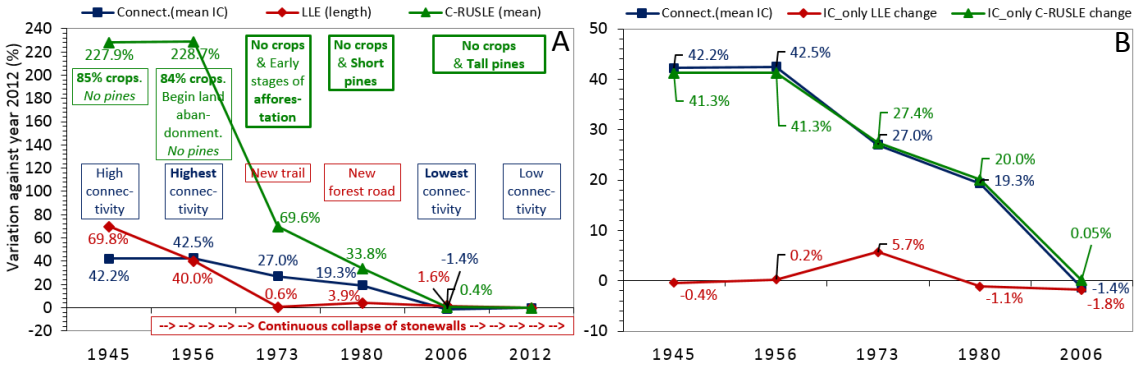

Table I. Land use characteristics and average values of the C-RUSLE factor for each scenario and map, and description and length of the linear landscape elements.

Scenario	Land use and land cover		Linear landscape elements	
	Description	C-RUSLE	Length	Description
1945	85% surface as cereal fields. Trees only appeared near the stream.	*0.2752 **0.0710 ***227.9%	#5216.9 ##4550.6 ###666.3 ***69.8%	2 trails. Most stonewalls and terraces well preserved: few breakpoints.
1956	84% surface as cereal fields. First abandoned fields near the divide. Trees only appeared near the stream.	*0.2747 **0.0711 ***228.7%	#4302.7 ##3636.4 ###666.3 ***40.0%	2 trails. Many small breakpoints in the stonewalls and terraces.
1973	Afforestation (59% of total surface): early stage, short pines (ca. 1 m height). Low dense scrublands.	*0.1418 **0.0987 ***69.6%	#3090.9 ##2225.9 ###865.0 ***0.6%	3 trails: 2 old plus 1 new linked to the afforestation. More breakpoints in the stonewalls and terraces.
1980	Afforestation: short-medium pines (ca. 2 m height). Low-medium dense scrublands. Very few areas with natural forest.	*0.1118 **0.1209 ***33.8%	#3193.0 ##1847.4 ###1345.6 ***3.9%	1 new forest road and 3 trails. More breakpoints in the stonewalls and terraces.
2006	Afforestation: tall pines (ca. 6.1 m height). 3 recent abandoned fields. Medium-dense scrublands. Small areas with natural forested areas.	*0.0839 **0.1388 ***0.4%	#3121.5 ##1606.6 ###1514.9 ***1.6%	1 forest road and 3 trails (2 old, 1 new and 1 abandoned). Many breakpoints in the stonewalls and terraces.
2012	Afforestation: tall pines (ca. 6.3 m height on average). 3 recent abandoned fields. Dense scrublands.	*0.0836 **0.1388	#3073.0 ##1558.1 ###1514.9	1 forest road and 3 trails. Many breakpoints in the stonewalls and terraces.

*mean and **standard deviation values; ***change related to the value in 2012; #total length (in meters) of all linear elements; ##total length (m) of all stonewalls and terraces; ###total length (m) of all trails and the forest road.

Table II. Values of runoff connectivity for the current scenario (year 2012) in the main physiographic and land use units, calculated with the three flow accumulation algorithms.

Algorithm	IC value	Total area	Hillslopes*	LLEs**	Stream and gullies	Upslope forest road$	Road and trails	Downslope forest road$	Afforested area
MD	mean	-4.0878	-4.2086	-2.5305	-3.0340	-4.3163	-2.1004	-3.8535	-4.4902
	sd	0.9816	0.8497	1.4182	1.1023	0.8733	1.2867	0.9705	0.6601
MD8	mean	-4.0858	-4.2073	-2.4965	-3.0524	-4.3080	-2.0535	-3.8627	-4.4910
	sd	1.0150	0.8844	1.4620	1.1362	0.9115	1.3356	0.9996	0.7101
D8	mean	-4.5097	-4.6639	-2.5180	-3.1666	-4.7416	-2.0338	-4.2819	-5.0798
	sd	1.0873	0.9150	1.4508	1.1563	0.9461	1.2596	1.1069	0.6056

*Excluding all LLEs; **all types of LLEs; $including afforested areas.

Table III. Values of runoff connectivity in the 5 past scenarios and in the main landscape units. Length of the flow path lines and values of the local changes (eight surrounding pixels) in connectivity.

Scenario (year)	Length FPL (m)#	Local change IC	IC value	Total area	Hillslopes*	LLE-wall**	LLE-T&R***	Stream and gullies
1945	##18.7	##0.0285	mean	-2.3602	-2.370	-2.614	-1.517	-2.018
	###281.1		sd	0.6193	0.594	0.829	0.904	0.674
	$-17.6%	$11.2%	change$	42.2%	43.7%	22.1%	26.1%	33.9%
1956	##20.5	##0.0280	mean	-2.3495	-2.364	-2.592	-1.441	-1.949
	###281.1		sd	0.6253	0.599	0.838	0.936	0.671
	$-9.6%	$9.5%	change$	42.5%	43.8%	22.7%	29.8%	36.1%
	$$9.8%	$$-1.5%	change$$	0.5%	0.3%	0.8%	5.0%	3.4%
1973	##23.4	##0.0262	mean	-2.9835	-3.021	-2.857	-1.861	-2.447
	###267.0		sd	0.6447	0.601	0.922	1.049	0.804
	$3.1%	$2.2%	change$	27.0%	28.2%	14.8%	9.4%	19.8%
	$$14.0%	$$-6.7%	change$$	-27.0%	-27.8%	-10.2%	-29.1%	-25.6%
1980	##22.5	##0.0257	mean	-3.2980	-3.367	-3.054	-1.979	-2.556
	###217.5		sd	0.7319	0.657	0.980	1.062	0.857
	$-0.6%	$0.3%	change$	19.3%	20.0%	9.0%	3.6%	16.3%
	$$-3.6%	$$-1.9%	change$$	-10.5%	-11.4%	-6.9%	-6.3%	-4.4%
2006	##22.4	##0.0264	mean	-4.1431	-4.257	-3.553	-2.267	-3.131
	###203.5		sd	0.9816	0.859	1.260	1.363	1.105
	$-1.3%	$3.2%	change$	-1.4%	-1.2%	-5.9%	-10.4%	-2.6%
	$$-0.7%	$$2.9%	change$$	-25.6%	-26.4%	-16.3%	-14.5%	-22.5%

#Length of the flow path lines (FPL) excluding the main stream; ##mean and ###maximum values; $Change compared with the scenario 2012; $$Change compared with the previous scenario; *Excluding all LLEs, the stream and the gullies; **Only stonewalls and terraces; ***Only trails and forest road.